Electronic Supplementary Information

One-step Synthesis of Ultrathin α-$Co(OH)_2$ Nanomeshes and Their High Electrocatalytic Activity toward the Oxygen Evolution Reaction

Bingxing Zhang,[a] Jianling Zhang,*[a] Xiuniang Tan,[a] Dongxing Tan,[a] Jinbiao Shi,[a] Fanyu Zhang,[a] Lifei Liu,[a] Zhuizhui Su,[a] Buxing Han,[a] Lirong Zheng[b] and Jing Zhang[b]

[a]Beijing National Laboratory for Molecular Sciences, CAS Key Laboratory of Colloid and Interface and Thermodynamics, Institute of Chemistry, Chinese Academy of Sciences, University of Chinese Academy of Sciences, China

[b]Beijing Synchrotron Radiation Facility (BSRF), Institute of High Energy Physics, Chinese Academy of Sciences, China

1. Experimental Section

Materials. $Co(NO_3)_2 \cdot 6H_2O$ (A. R. grade), $CoCl_2 \cdot 6H_2O$ (A. R. grade), $Ni(NO_3)_2 \cdot 6H_2O$ (A. R. grade), anhydrous $MnCl_2$ (A. R. grade), $Cu(NO_3)_2 \cdot 3H_2O$ (A. R. grade) and Potassium hydroxide (A. R. grade) were provided by Sinopharm Chemical Reagent Co., Ltd. Methylimidazole (MIM, 99%) was obtained from J&K Scientific Ltd. Nafion D-521 dispersion (5% w/w in water and 1-propanol, >0.92 meg/g exchange capacity) and hexamethylenetetramine (HMT) (>99%) was purchased from Alfa Aesar China Co., Ltd. Deionized water, methanol (A. R. grade), ethanol (A. R. grade) and N_2 (>99.9%) were provided by Beijing Analysis Instrument Factory.

α-$Co(OH)_2$ nanomesh synthesis. MIM (0.25 g) and $Co(NO_3)_2 \cdot 6H_2O$ (0.45 g) were respectively dissolved in 12 mL CH_3OH/H_2O (1/1 v/v) and 12 mL CH_3OH/H_2O (1/1 v/v) mixed solvent under ultrasound for 20 min. Then the above two solutions were mixed immediately (pH ≈ 9) and kept at room temperature for 24 h. After reaction, the suspension was separated by centrifugation and the solid was washed thoroughly with ethanol and finally dried at 60 °C under vacuum overnight. The yield of α-$Co(OH)_2$ product was 71.3% based on Co ions. The control sample was synthesized at the temperatures and solvent systems adjusted by $NH_3 \cdot H_2O$ to pH ≈ 9.

Bulk α-$Co(OH)_2$ synthesis. $CoCl_2$ (1.19 g) and HMT (1.68 g) were dissolved in water (90 mL) and ethanol (10 mL) solution. The above solution was refluxed at 95 °C for 1 h. The product was collected by centrifugation followed by washing with deionized water and ethanol and drying at 60 °C under vacuum.

α-$Co(OH)_2$ nanosheet synthesis. The above bulk α-$Co(OH)_2$ product was dispersed in 100 mL ethanol and sonicated for 4 h. Then the exfoliated nanosheets were collected by centrifuging the supernatant at 10000 rpm for 5 min, followed by washing with deionized water and ethanol and drying at 60 °C under vacuum.

Bimetallic hydroxide nanomesh synthesis. The synthesis procedure was similar to the α-$Co(OH)_2$ nanomesh synthesis except the 0.045 g $Ni(NO_3)_2 \cdot 6H_2O$, anhydrous $MnCl_2$ and $Cu(NO_3)_2 \cdot 3H_2O$ were added to the mixture for the (Ni, Co)-hydroxides, (Mn, Co)-hydroxides, (Cu, Co)-hydroxides synthesis, respectively.

Material characterizations. Powder X-ray diffraction pattern was performed on a Rigaku D/max-2500 diffractometer with Cu Kα radiation (λ = 1.5418 Å) at 40 kV and 200 mA. The ethanolic suspensions of products were collected and dropped on clean glass for XRD characterization. The morphologies were characterized by SEM (HITACHI S-4800), TEM (JEOL-1010) operated at 100 kV and HRTEM (JEOL-2100F) operated at 200 kV. AFM measurements were performed on a tapping-mode atomic force microscope (Nanoscope IIIa, Digital Instruments, Santa Barbara, CA) with a silicon cantilever probes. XPS was determined by VG Scientific ESCALab220i-XL spectrometer using Al Kα radiation. The 500 μm X-ray spot was used. The base pressure in the analysis chamber was about 3×10^{-10} mbar. The porosity properties were gained from N_2 adsorption-desorption analysis using a Micromeritics ASAP 2020M system. The UV-visible diffuse reflectance spectra were recorded with a UV-visible spectrophotometer (UV-2550, Shimadzu, Japan). Electron spin resonance (ESR) spectra were collected on a Bruker ESP-300 spectrometer. The XAFS experiment was carried out at Beamline 1W1B at BSRF. Data of XAFS were processed using the Athena and Artemis programs of thee IFEFFIT package based on FEFF 6. Prior to merging, the absorption spectrum was aligned to the first and largest peak in the smoothed first derivative of the spectrum, followed by background subtraction and normalization. Data were processed with k^2-weighting and an Rbkg value of 1.0. Merged data sets were aligned to the largest peak in the first derivative of the adsorption spectrum. Normalized μ(E) data were obtained directly from the Athena program of the IFEFFIT package.

Electrochemical measurements. The catalyst dispersion or ink was prepared using mixture of 0.5 mL ethanol, 0.02 mL 5 wt% Nafion solution and 2 mg catalyst followed by ultrasonication for 2 h. Then, 10 μL of the ink was uniformly loaded onto a glassy-carbon electrode (diameter = 0.4 cm), which was used as the working electrode with a loading of 0.32 mg cm^{-2} catalysts.

The electrochemical tests were performed in a three-electrode electrochemical cell (Pine Instruments) using Pt mesh and Ag/AgCl electrode as counter electrode and reference electrode, respectively. Potassium hydroxide aqueous solution (1 M) with

high-purity N_2 gas bubbled at least 30 min was used as the electrolyte. All potentials measured were calibrated to the reversible hydrogen electrode (RHE) using the following equation: $E_{RHE} = E_{Ag/AgCl} + 0.197\ V + 0.059\ pH$. For oxygen evolution reaction (OER) tests, the polarization curves and Tafel plots were recorded at scan rates of 10 mV s^{-1} and 1 mV s^{-1}, respectively. The rotation speeds conducted at 1600 r.p.m. The solution impedance (R) of 1 M KOH measured was 6.9 Ω at room temperature. All polarization curves were corrected with 100% iR-compensation. The impedance spectra were recorded under an open-circuit voltage in the frequency range from 10^5 to 0.1 Hz with a 5 mV amplitude.

2. Results and Discussion

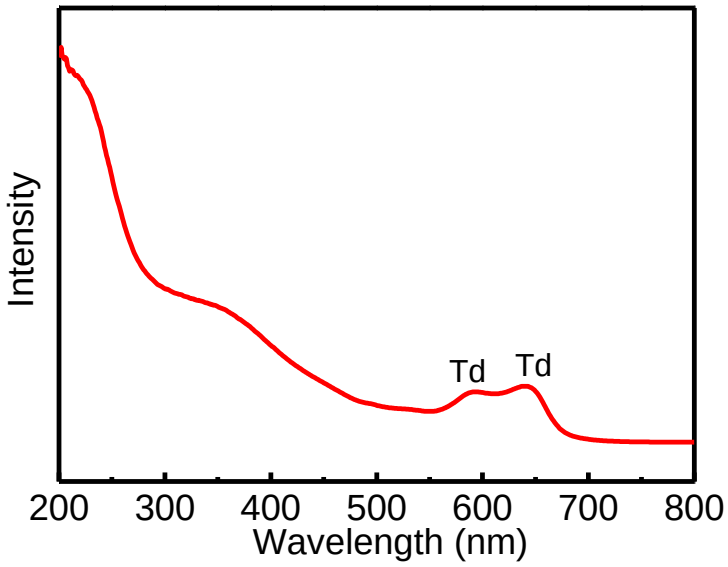

Fig. S1. UV-Vis absorption spectra of α-$Co(OH)_2$ nanomesh. It show a broad absorption peak located at ~360 nm that can be attributed to the presence of Co^{2+}_{Oh} sites. The two peaks at ~590 and ~640 nm indicate the presence of the Co^{2+}_{Td} site, which are in favor of the formation of the active CoOOH sites during OER.[1] This also confirms the successful preparation of α-$Co(OH)_2$.[2]

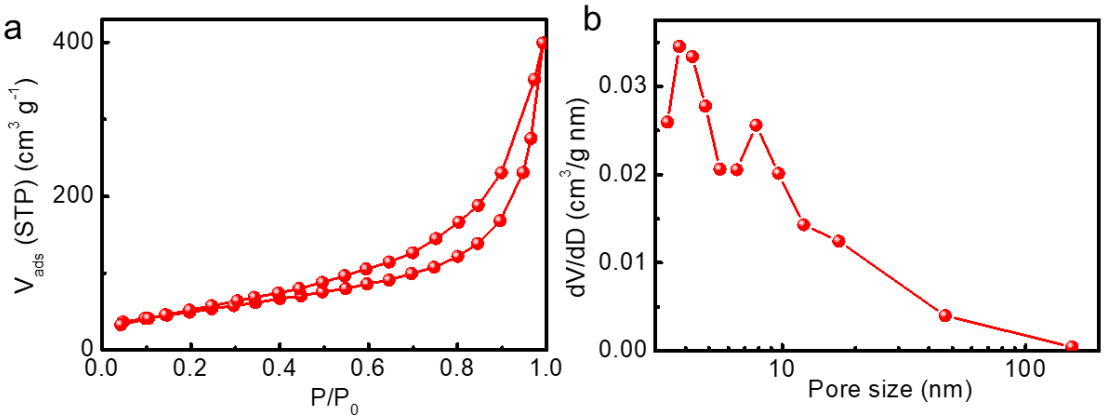

Fig. S2. N_2 adsorption/desorption isotherms (a) pore size distribution curve (b) of α-$Co(OH)_2$ nanomesh.

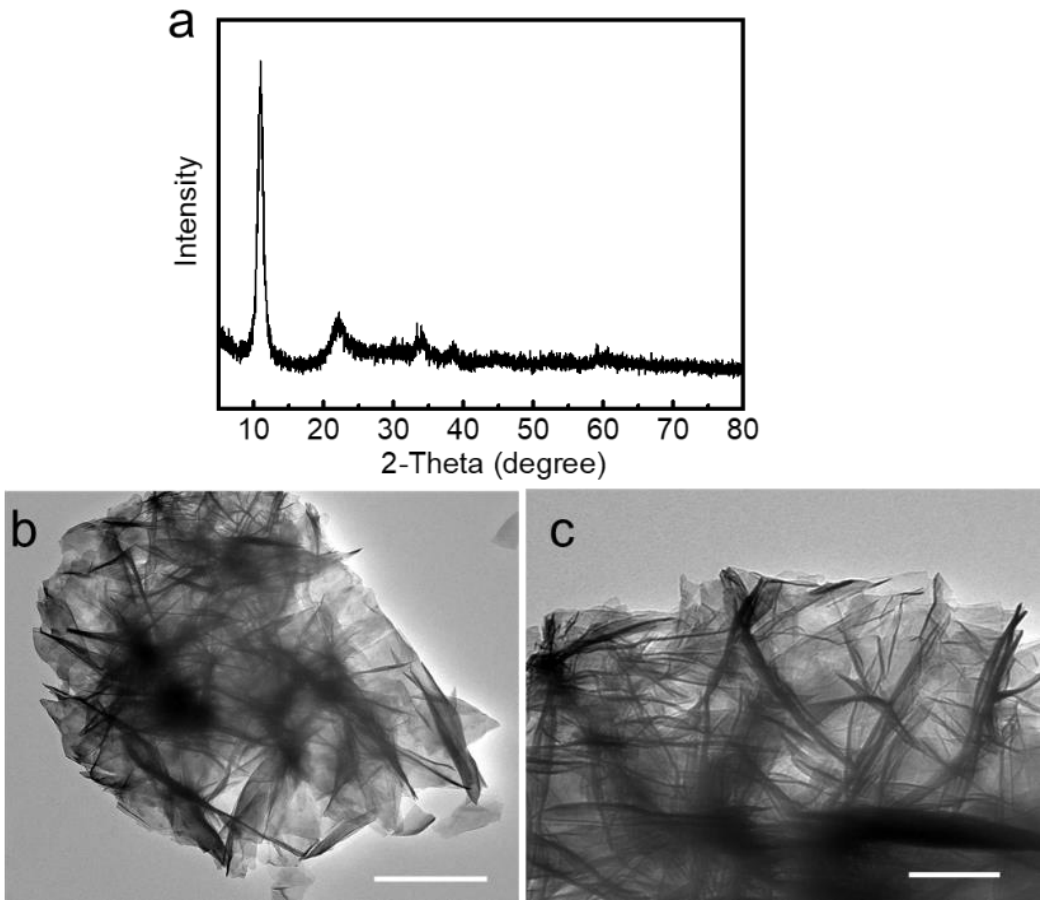

Fig. S3. XRD pattern (a) and TEM images (b, c) of α-$Co(OH)_2$ nanosheet. Scale bar, 1 μm in panel b and 200 nm in panel c.

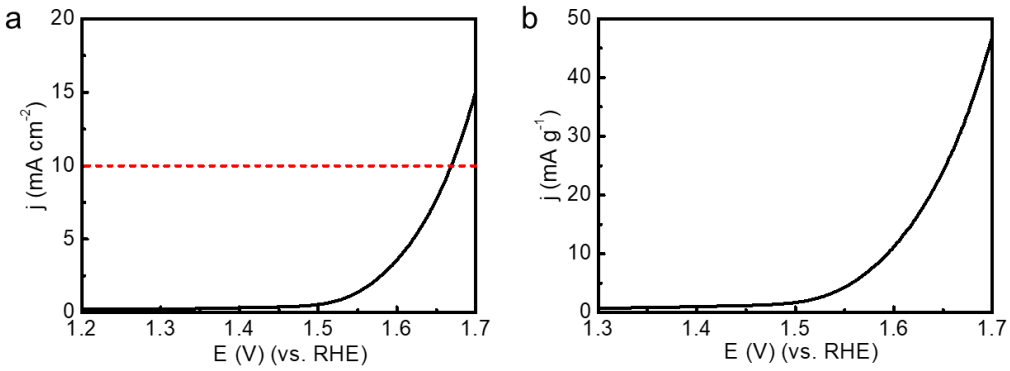

Fig. S4. Linear sweep voltammetry curves (a) and mass activity comparison of the bulk α-$Co(OH)_2$. The bulk α-$Co(OH)_2$ presents current density of 10 $mA \cdot cm^{-2}$ with an overpotential of 439 mV and a mass activity of 2.9 $A \cdot g^{-1}$ when applying an overpotential of 303 mV.

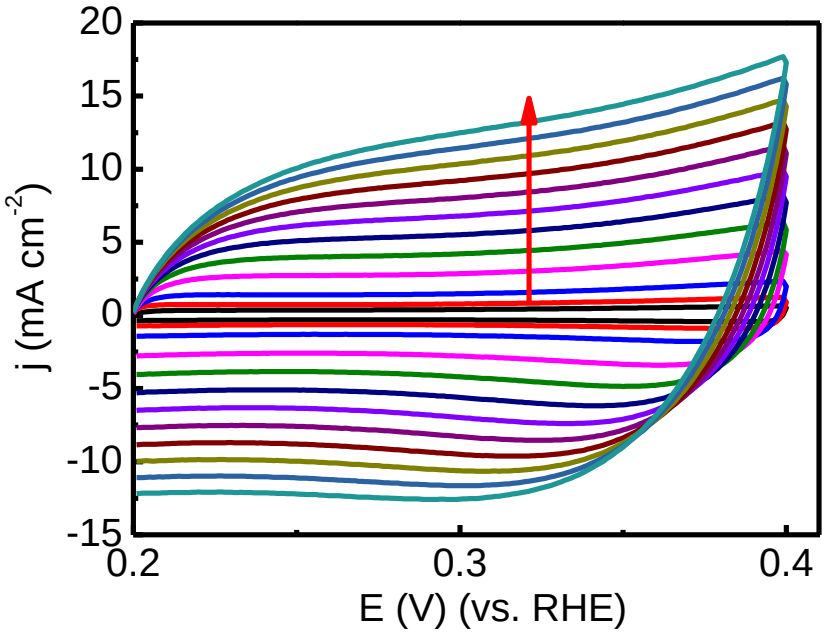

Fig. S5. Cyclic voltammograms of α-$Co(OH)_2$ nanomesh at various scan rates of 5, 10, 20, 40, 60, 80, 100, 120, 140, 160, 180 and 200 mV s^{-1}.

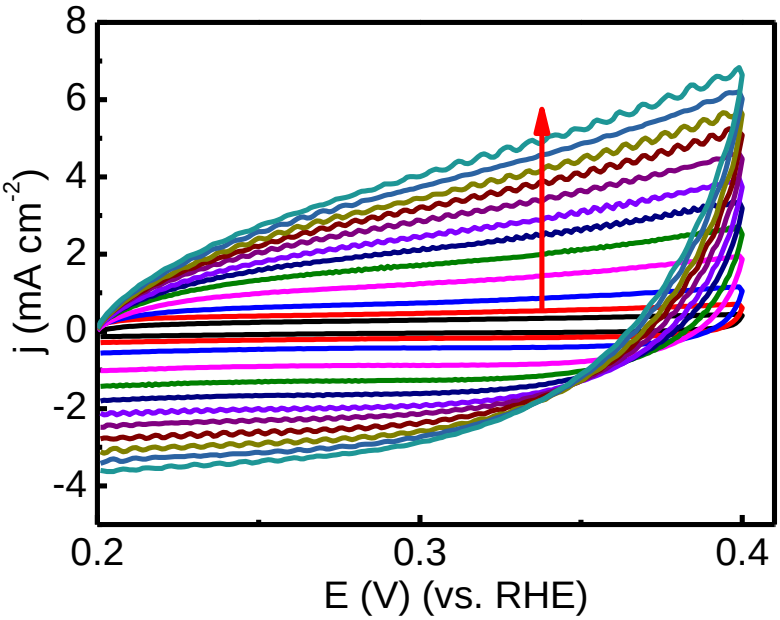

.

Fig. S6. Cyclic voltammograms of α-$Co(OH)_2$ nanosheet at various scan rates of 5, 10, 20, 40, 60, 80, 100, 120, 140, 160, 180 and 200 mV s^{-1}.

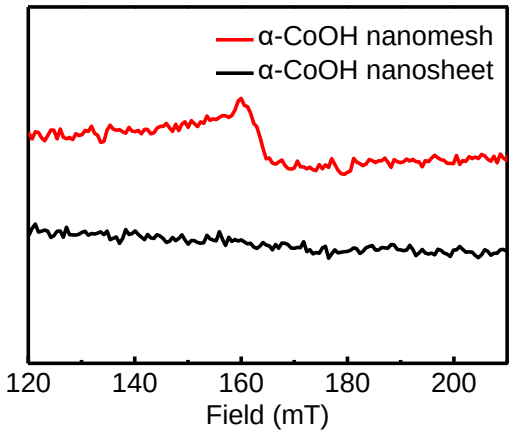

Fig. S7. ESR spectra of α-$Co(OH)_2$ nanomeshes and α-$Co(OH)_2$ nanosheets. ESR spectra reveal the difference between α-$Co(OH)_2$ nanomeshes and α-$Co(OH)_2$ nanosheets. α-$Co(OH)_2$ nanomeshes give a major feature with a g-value of 4.3. It may be assigned to the lower symmetry of the structures and oxygen vacancy.[3,4] Such signal was not observed for α-$Co(OH)_2$ nanosheets.

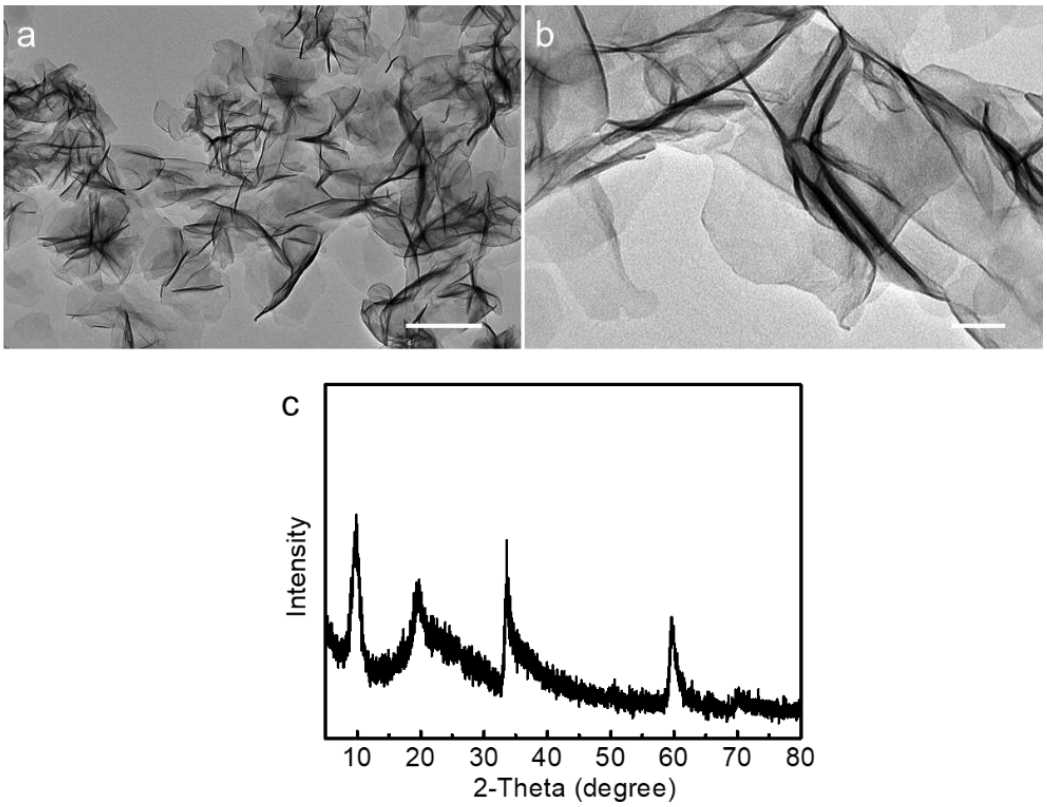

Fig. S8. TEM images (a, b) and XRD pattern (c) of the product synthesized in CH_3OH/H_2O system without MIM (pH≈9 adjusted by $NH_3 \cdot H_2O$). Scare bar, 200 nm in panel a and 50 nm in panel b.

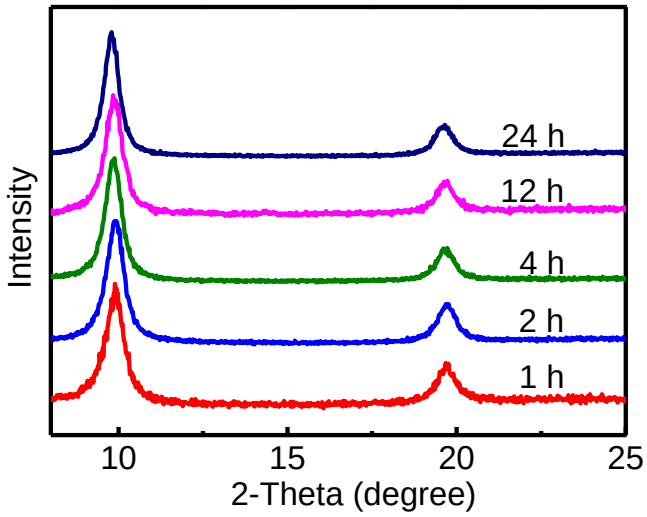

Fig. S9. XRD patterns of the α-$Co(OH)_2$ nanomesh synthesized with different reaction time.

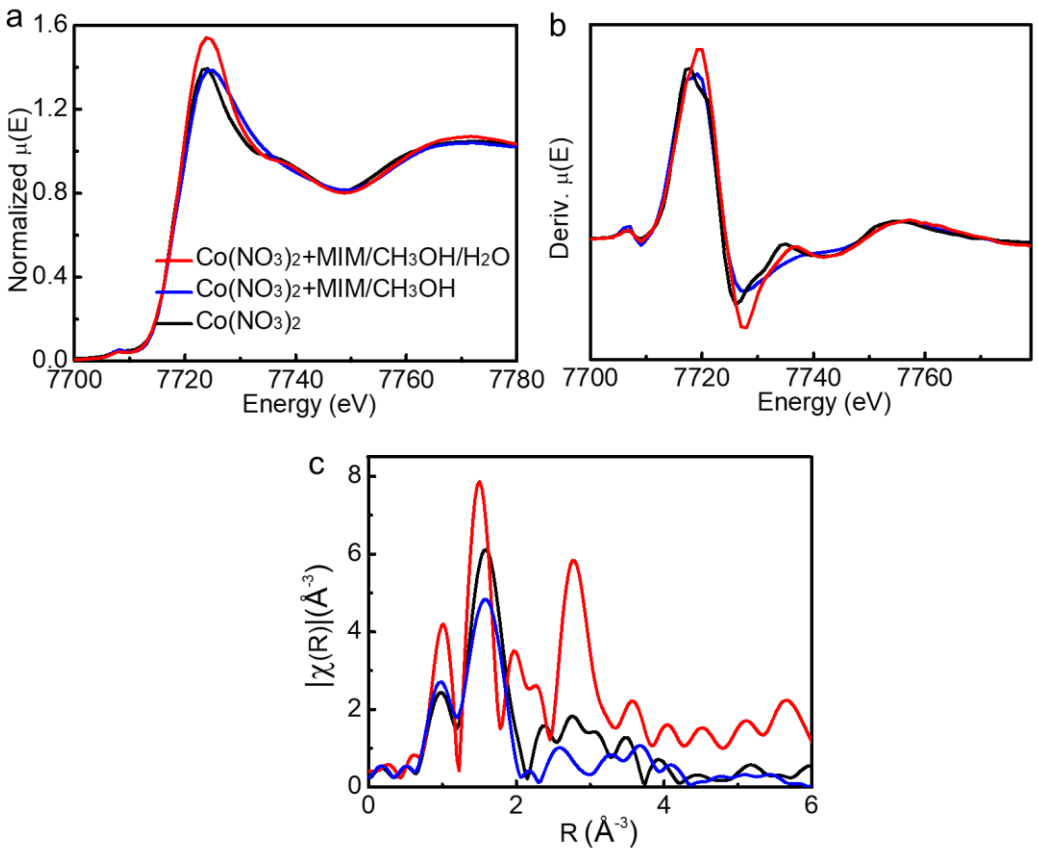

Fig. S10. EXAFS spectra at Co k-edge of solid $Co(NO_3)_2 \cdot 6H_2O$ (black) and dissolved $Co(NO_3)_2 \cdot 6H_2O$ in $MIM/CH_3OH/H_2O$ (red) and MIM/CH_3OH (blue), respectively. The XANES of $Co(NO_3)_2 \cdot 6H_2O$ (starting material with octahedral (O_h) coordination at Co center) before and after dissolved in $MIM/CH_3OH/H_2O$ and MIM/CH_3OH were investigated (Fig. S5a). The dissolved Co ions in $MIM/CH_3OH/H_2O$ system has higher white line intensity (first resonance after the edge) than the other two samples. Moreover, the increased intensity of white line and a small decrease of the pre-edge feature around 7708 eV for Co ions in $MIM/CH_3OH/H_2O$ system can be further certified by derivated XANES spectra (Fig. S5b). There is no doubt that there are more Co-MIM coordination in MIM/Ch_3OH system than that in $MIM/CH_3OH/H_2O$ system due to nearly no OH^- existence in the former. The results manifest that more MIM ligands coordinated to Co ions will decrease their white line intensity. Because the Co-MIM coordination may possess tetrahedral (T_d) coordination structure, which possess prominent pre-edge feature but weak white line intensity due to the decreased multiple

scattering for a T_d coordination compared with O_h geometry.[5] The extended X-ray absorption fine structure (EXAFS) spectrum (Fig. S5c) can further demonstrate that Co ions in MIM/Ch_3OH system with more Co-MIM coordination have lower Co-O or Co-N (around 1.56 Å) coordination compared with that in MIM/Ch_3OH/H_2O system.

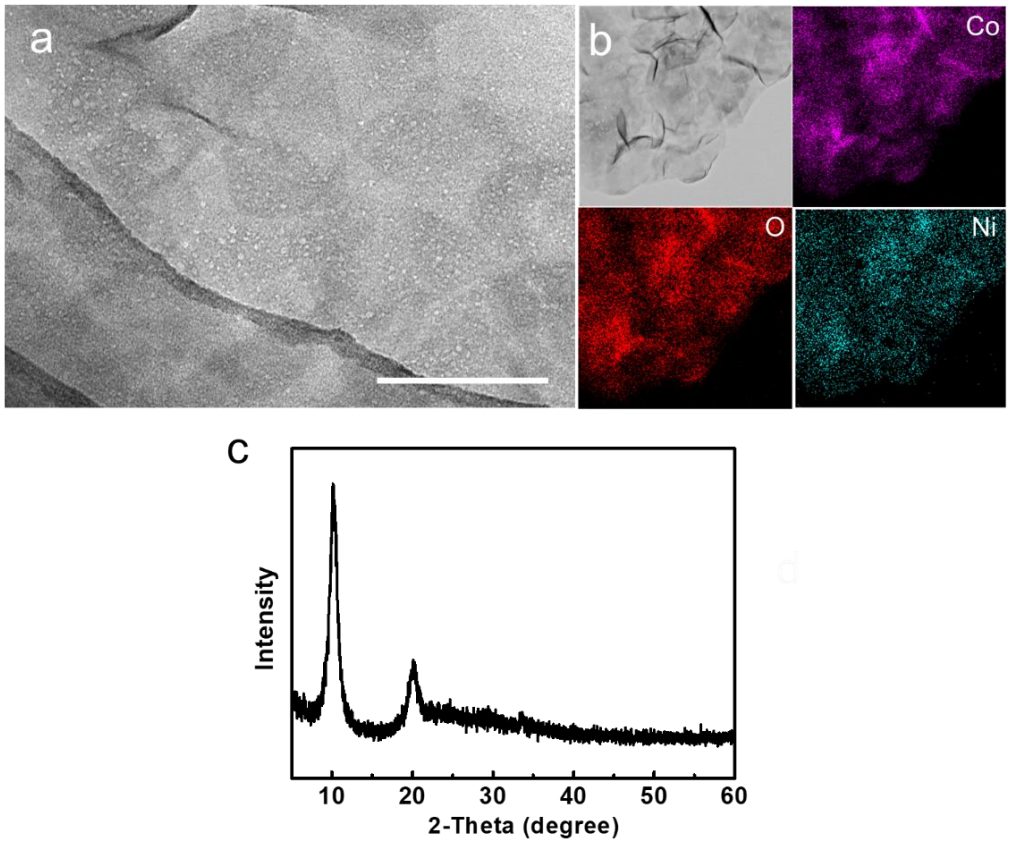

Fig. S11. TEM image (a), elemental mapping (b) and XRD pattern (c) of (Ni, Co)-hydroxides nanomesh. Scale bar, 100 nm. The obtained Co/Ni weight ratio is determined to be about 10/1.

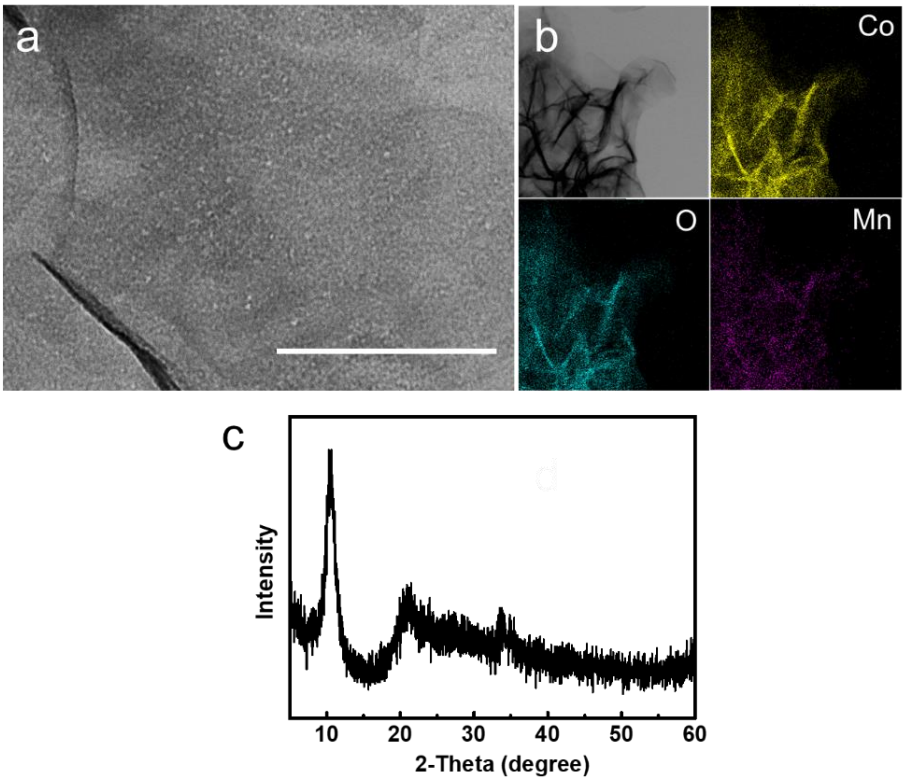

Fig. S12. TEM image (a), elemental mapping (b) and XRD pattern (c) of (Mn, Co)-hydroxides nanomesh. Scale bar, 100 nm. The obtained Co/Mn weight ratio is determined to be about 15/1.

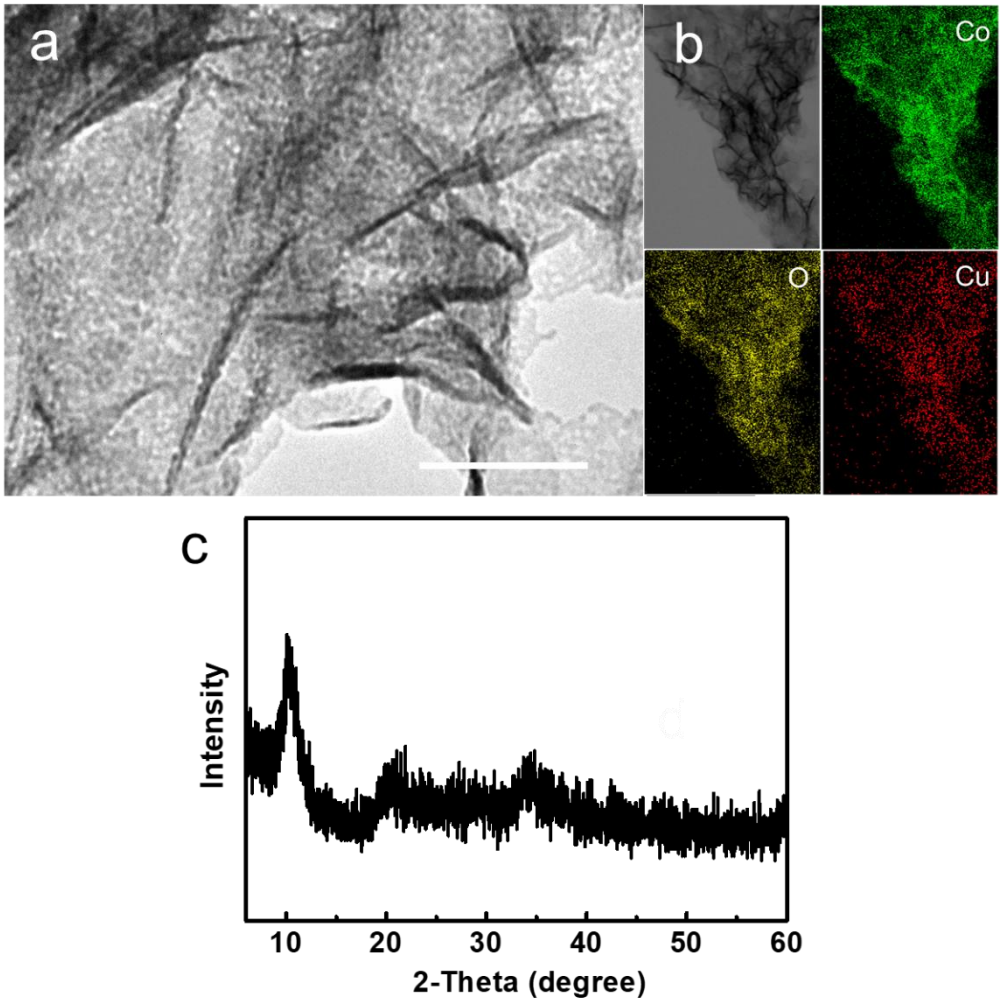

Fig. S13. TEM image (a), elemental mapping (b) and XRD pattern (c) of (Cu, Co)-hydroxides nanomesh. Scale bar, 50 nm. The obtained Co/Cu weight ratio is determined to be about 15/1.

Table S1. Comparison of OER performance of various reported electrocatalysts and this work. The presented catalysts are loaded on the GCE and the tested in 1M KOH electrolyte.

Electrocatalysts	Overpotential at current density of 10 $mA \cdot cm^{-2}$ (mV)	Ref.
α-$Co(OH)_2$ nanomesh	303	This work
NiCo LDHs	367	*Nano Lett.* **2015**, *15*, 1421.
Co phosphide/phosphate	300	*Adv. Mater*. **2015**, *27*, 3175.
γ-CoOOH NS*	300	*Angew. Chem. Int. Ed*. **2015**, *54*, 8722.
$Co(OH)_2$@Au	360	*J. Mater. Chem. A*. **2016**, *4*, 991.
Co-P/NC*	319	*Chem. Mater*. **2015**, *27*, 7636.
NiCo-HS@G	302	*Adv. Funct. Mater.* **2018**, *28*, 1704594.
$(Ln_{0.5}Ba_{0.5})CoO_{3-\delta}$	~350	*Nat. Commun*. **2013**, *4*, 2439.
$PrBa_{0.5}Sr_{0.5}Co_{1.5}Fe_{0.}5O_{5+\delta}$	~358	*Nat. Commun*. **2017**, *8*, 14586.
$Ni@[Ni^{(2+/3+)}Co_2(OH)_{6-7}]_x$	460	*Adv. Funct. Mater*. **2014**, *24*, 4698.
$Co(OH)_2$-Cl	380	*Dalton Trans*. **2017**, *46*, 10545-10548
LiNiCo-OH	340	*Nano Lett*. **2015**, *15*, 2498-2503.

Ultrathin CoMn-LDH	350	*J. Am. Chem. Soc*. **2014**, *136*, 16481-16484.
Co_3O_4@CoO SC	430	*Nat. Commun*. **2015**, *6*, 8106.
$NiCo_{2.7}OH$	350	*Adv. Energy Mater*. **2015**, *5*, 1401880.
Co/CoP-5	340	*Adv. Energy Mater.* **2017**, 1602355
CoO_x-ZIF	~320	*Adv. Funct. Mater.* **2017**, *27*, 1702546
$Zn_xCo_{3-x}O_4$-3:1	320	*J. Am. Chem. Soc.* **2012**, *134*, 17104.
$Co_3O_4/NiCo_2O_4$	340	*Energy Environ. Sci.* **2013**, *6*, 3553.
CoMn LDH	325	*J. Am. Chem. Soc.* **2014**, *136*, 16481.

References

[1] H.-Y. Wang, S.-F. Hung, H.-Y. Chen, T.-S. Chan, H. M. Chen, B. Liu, *J. Am. Chem. Soc.*, 2016, **138**, 36-39.

[2] R. Z. Ma, Z. P. Liu, K. Takada, K. Fukuda, Y. Ebina, Y. Bando, T. Sasaki, *Inorg. Chem.*, 2006, **45**, 3964-3969.

[3] F. M, Scaldini, M. C. R, Freitas, M. D, Reis, M. I, Yoshida, K, Krambrock, F. C, Machado, *New J. Chem.*, 2018, **42**, 1216-1222.

[4] Y. F, Zhao, Y. X, Zhao, G. I. N, Waterhouse, L. R, Zheng, X. Z, Cao, F, Teng, L. Z, Wu, C. H, Tung, D, O'Hare, T. R, Zhang, *Adv. Mater.* 2017, **29**, 1703828.

[5] B. Pattengale, S. Z. Yang, J. Ludwig, Z. Q. Huang, X. Y. Zhang, J. Huang, *J. Am. Chem. Soc.*, 2016, **138**, 8072-8075.